



**Next Generation Very Large Array Memo No. 126
August 2024**

**VLA – ngVLA transition: Comparison of two representative
fixed-mixed scale configurations to the current VLA**

C.L. Carilli

National Radio Astronomy Observatory, Socorro, NM, USA

Abstract

I have considered the question: how well does a single (fixed), mixed-scale configuration of the 27 VLA antennas involving baselines from D to A array, perform relative to the current individual VLA configurations (A,B,C,D)? I have employed two representative configurations: one with an emphasis on longer spacings (VLA-F), and the second with better short spacing coverage (VLA-G). Overall, it appears that getting within a factor 1.3 to 2, of the thermal noise performance of individual current VLA configurations is plausible with a mixed-configuration covering a wide range in baselines. The PSF sidelobes seem more challenging, with performance degraded by factors of 2 up to 6, relative to individual current VLA configurations. If the paramount science at the time of VLA to ngVLA transition requires very high dynamic range imaging of complex fields, the PSF sidelobe level may become the primary selection criterion for choosing the final configuration.

1 Introduction

The ngVLA Transition Advisory Group is considering what to do with the Very Large Array during the initial construction of the ngVLA (TAG report August 2024). The current plan is that, once the ngVLA has the sensitivity of the current VLA, corresponding to 30 antennas, then the VLA will be

decommissioned. During this initial phase of ngVLA construction, which could take up to 4 years, the desire is to continue operation of the VLA to maintain radio science capabilities in the USA, but possibly to reduce VLA operations demands by limiting options; one option of which is to discontinue reconfiguration.

If the 27 antennas of the VLA were to be set in one configuration for the transition period, two extreme can be considered. First, choose one of the current VLA configurations and focus on the highest profile science that can be done with that configuration. Examples are fixing the array in D array for low surface brightness work, or in A array for high resolution imaging. Second, put the array in a mixed-scale configuration that samples all the scales of the current VLA, but with reduced performance. The decision on these two alternatives will depend on the highest priorities of the science community at the time of transition (expected sometime around 2030), and hence the decision does not need to be, and indeed, cannot be, made today.

However, in preparation for the transition, it is important to address the general question: what is the performance loss for a mixed-scale configuration relative to the current VLA, given the need to cover D to A array baselines with only 27 antennas? In this memo, I consider two representative mixed-scale configurations. One emphasizes longer baselines, with only a marginal sampling of D array baselines. The second adds antennas on D-array scales, at the expense of the longer baselines. Again, the choice of optimal mixed-scale configuration, or single current configuration, will be dictated by the science priorities at the end of the decade. The two configurations considered herein provide a reasonable exercise in the performance of mixed-scale configurations, relative to the individual current VLA configurations.

As performance metrics, I adopt the rms thermal noise, the maximum positive and negative sidelobes of the PSF, and the rms of the PSF sidelobes. The thermal noise represents the ultimate limit to the sensitivity of the configuration at the target spatial resolution, dictated by the uv-weighting required to obtain the target resolution. The PSF sidelobes become relevant when imaging complex fields with bright sources, where image dynamic range may become the limitation. In each case, we compare the mixed-scale results to the relevant VLA configuration (A,B,C,D).¹

¹Note that I consider only one declination. The squeezing of the PSF N-S with declination for any configuration is similar, to first order. Non-linear configuration dependent phenomena with declination, such as shadowing, are second-order and beyond the scope or the need of this design study.

2 Simulations

The CASA simulator is employed for a 30min and an 8 hour observation of a source at $+40^\circ$ declination, at a frequency of 8 GHz. I start with the four current VLA individual configurations (A (30km), B(10 km), C (3 km), D (1km)), using Natural weighting in each case to obtain the 'reference' observation thermal noise and point spread function (PSF) for each. At 8 GHz, the corresponding PSF FWHM values are roughly 0.3", 0.9", 3", and 10", respectively.

I then consider the two mixed-scale configurations and employ TCLEAN, adjusting the robust weighting and uvtaper in each case to obtain a PSF with close to the same FWHM (within a few percent), of each current NA-weighted VLA configuration, based on the Gaussian fitting to the PSF in TCLEAN.

Noise is added to each simulated data set. Since only comparative measurements are considered, unit noise is added to each visibility using setnoise in CASA.

The antenna distribution for the two mixed-scale configurations are shown in Figure 1. The first is the VLA-F configuration from Wrobel & Walker (2022 ngVLA memo 97). The second configuration, which I designate VLA-G, is a mix of antennas from D to A array spacings, but includes more D-array spacings than VLA-F

The uv-coverage for VLA-F and VLA-G are shown in Figure 2. Both the full array (20 km radii), and the inner array (2 km radii) are shown. VLA-F has good coverage of the long spacings, but only 6 antennas at radii < 600 m, and hence poor coverage on D-array baselines. The VLA-G has 11 antennas at radii < 600 m, and hence better uv-coverage on D-array baselines, at the expense of more sparse coverage on the longest baselines.

3 Results

Table 1 lists the results for the PSF FWHM for all configurations, and the weighting and tapering used to achieve those values. Also listed are the rms noise levels in the images (again, normalized to a unit noise level for each visibility), the peak negative and positive sidelobes of the PSF, and the rms sidelobe levels derived at radii from $2\times$ to $20\times$ the FWHM. Figures 3-10 show the PSF images for each configuration and weighting.²

²Note that the PSF for each VLA configuration (A,B,C,D) are all very similar, with simply a scale change, because the VLA configurations are roughly a self-similar transform

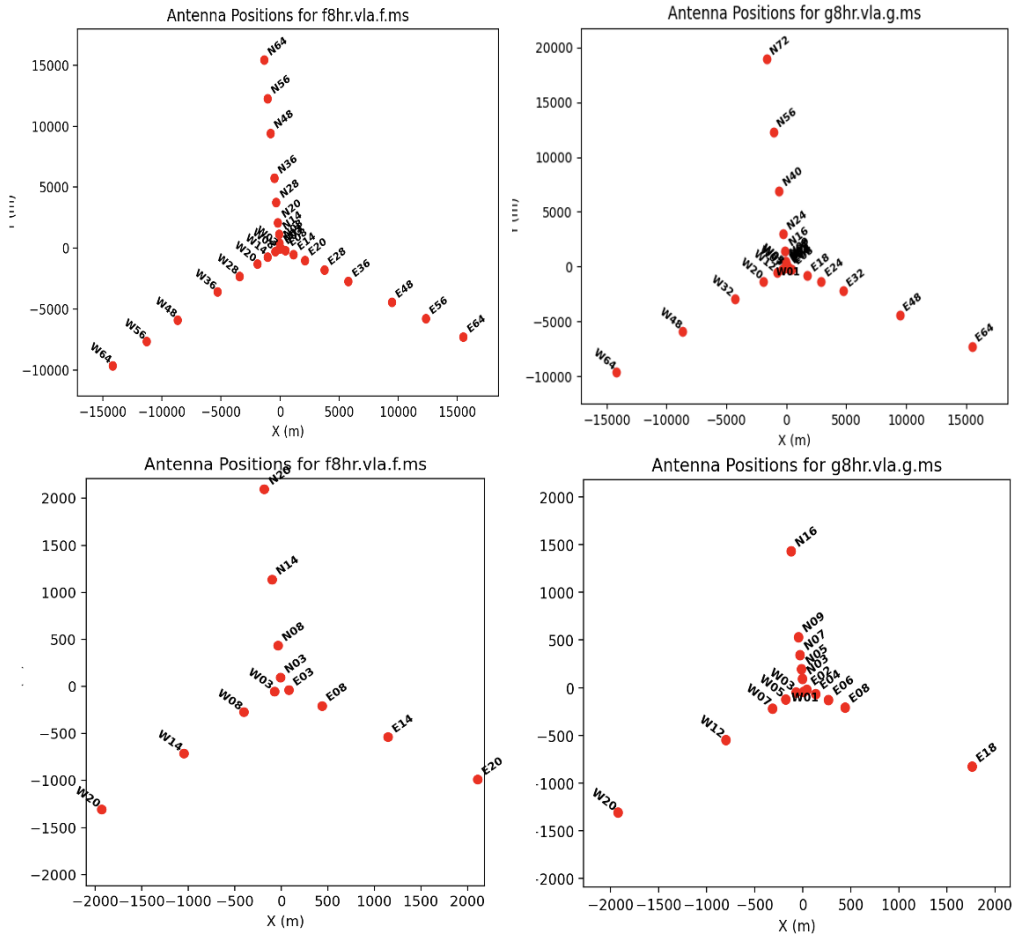


Figure 1: Top: plots of the antenna distribution to radii of 20 km. Left is VLA-F and right is VLA-G. Lower: Same to radii of 2 km.

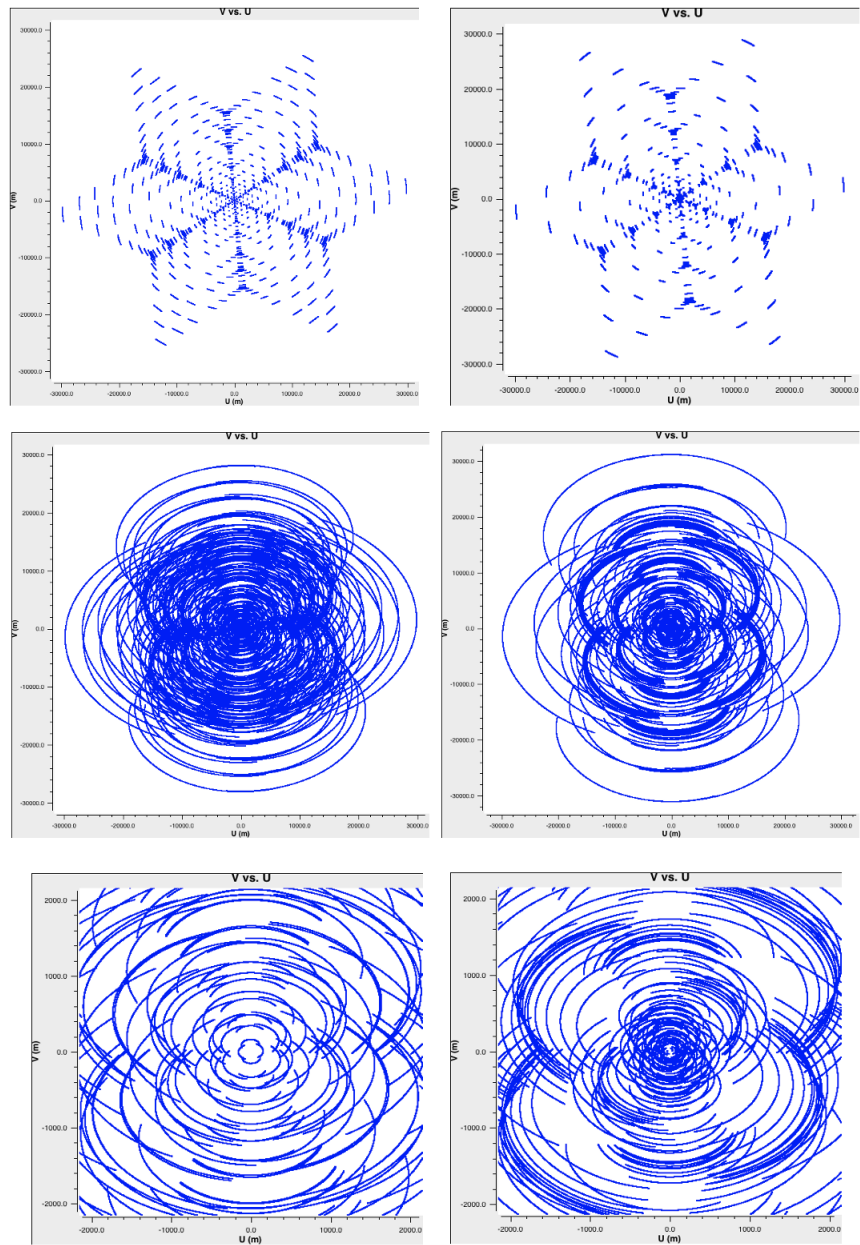


Figure 2: Top left: UV coverage VLA-F and right is VLA-G for a 30min integration. Middle: same but for 8 hour integration. Bottom: UV coverage for short spacings in 8hrs.

Table 1: Beam Sizes, Sensitivities, and Sidelobes

Data	Weight	Taper arcsec	FWHM arcsec	rms mJy	SL_{max}	SL_{min}	SL(rms)
0.5 Hours							
VLA A	NA	0	$0.279 \times 0.258, -3.1^\circ$	4.9	0.250	-0.038	0.032
VLA F	R=-2	0	$0.279 \times 0.242, -3.8^\circ$	6.2	0.428	-0.139	0.036
VLA G	R=-2	0	$0.271 \times 0.259, -76.8^\circ$	6.7	0.52	-0.21	0.067
VLA B	NA	0	$0.911 \times 0.848, -2.3^\circ$	4.9	0.278	-0.038	0.029
VLA F	R=0.5	0.8	$0.924 \times 0.894, -1.2^\circ$	7.8	0.390	-0.110	0.042
VLA G	R=0	0.7	$1.050 \times 0.833, 18.5^\circ$	7.3	0.48	-0.14	0.041
VLA C	NA	0	$2.967 \times 2.730, -3.0^\circ$	4.9	0.280	-0.038	0.030
VLA F	R=1.5	2.4	$2.870 \times 2.839, 68.3^\circ$	12.3	0.46	-0.14	0.078
VLA G	R=0.5	2.3	$3.079 \times 2.859, 19.1^\circ$	8.4	0.41	-0.12	0.047
VLA D	NA	0	$9.693 \times 8.953, -3.0^\circ$	4.9	0.308	-0.038	0.035
VLA F	R=2	8.8	$9.412 \times 9.205, 78.3^\circ$	21.0	0.790	-0.284	0.18
VLA G	R=2	6.0	$9.84 \times 8.94, -73.3^\circ$	10.0	0.29	-0.11	0.070
8 Hours							
VLA A	NA	0	$0.293 \times 0.275, -88.2^\circ$	1.2	0.034	-0.020	0.0083
VLA F	R=0	0	$0.284 \times 0.272, -85.9^\circ$	1.5	0.102	-0.040	0.0092
VLA G	R=-2	0	$0.299 \times 0.245, 88.1^\circ$	1.77	0.11	-0.083	0.017
VLA B	NA	0	$0.959 \times 0.901, -88.5^\circ$	1.2	0.032	-0.020	0.0080
VLA F	R=0	0.95	$0.958 \times 0.934, -7.4^\circ$	2.2	0.068	-0.046	0.010
VLA G	R=0	0.8	$0.995 \times 0.94, 41.4$	1.91	0.11	-0.066	0.011
VLA C	NA	0	$3.081 \times 2.926, -87.4^\circ$	1.2	0.029	-0.021	0.0084
VLA F	R=1	2.9	$3.076 \times 3.025, -86.9^\circ$	3.3	0.090	-0.069	0.021
VLA G	R=0.5	2.7	$3.047 \times 2.992, 74.2$	2.27	0.17	-0.056	0.011
VLA D	NA	0	$10.099 \times 9.569, -87.9^\circ$	1.2	0.030	-0.026	0.015
VLA F	R=2	9.5	$10.122 \times 9.750, 87.9^\circ$	7.4	0.217	-0.181	0.070
VLA G	R=2	6.5	$10.69 \times 9.50, -81.9^\circ$	2.74	0.082	-0.058	0.024

Figure 11 shows the rms noise values for two mixed configurations from Table 1, normalized by the rms value achieved for the individual current VLA configurations. The rms values are plotted against the nominal resolution of each configuration/weighting test. At the highest resolution, the VLA-F configuration has 26% higher noise level than the VLA-A. VLA-G is a bit worse (36% higher than VLA-A). As the resolution gets lower, the relative performance of the VLA-F degrades substantially, such that at VLA-D resolution (10"), the noise level of VLA-F relative to VLA-D is a factor 5 higher. The VLA-G noise level at D array resolution is only a factor 2 higher than VLA-D.

The improved noise performance of VLA-G at VLA-D resolution is simply due to the fact that almost half the antennas are within 1km radius of the center. Further, VLA-G noise does not suffer dramatically at the highest resolution since the inner antennas still participate, although with a reducing weighting. The behaviour is similar to the ngVLA with the large core. Even tapered to the highest resolution, the ngVLA sensitivity loss is at worst a factor two relative to NA of the full configuration (Rosero & Carilli 2022 ngVLA memo 106).

The peak positive and negative sidelobe levels for the PSF vs. configuration resolution are shown in Figure 12 and 13. At the highest resolution (VLA-A) for the 30min integration, VLA-F has a peak positive sidelobe a factor 1.7 higher than VLA-A, and a peak negative sidelobe higher by a factor 3.7. The values for VLA-G are 2.1 and 5.5. As expected, the VLA-G PSF quality at VLA-A resolution is substantially worse than VLA-F due to the fewer antennas on long baselines. At the lowest resolution (VLA-D), the corresponding peak positive and negative sidelobe ratios with respect to VLA-D for VLA-F are 2.6 and 7.5, while those for VLA-G are 1 and 2.9.

Figure 14 shows the rms of the PSF sidelobes from radii = $2 \times$ FWHM to $20 \times$ FWHM. The trend is the same as for the peak sidelobes. VLA-F performs almost as well as A configuration (within 12%), but performs poorly at D configuration resolution (factor 5 worse than VLA-D; see Figure 6b). For VLA-G, the rms sidelobes are about a factor 2 worse than both VLA A and D configurations.

The most dramatic degradations of PSF performance occur for the 30min exposure for VLA-F at the D array resolution (Figure 6b), where the paucity of antennas on the D-array scales (6 total), leads to a peak 79% sidelobe, and for VLA-G at VLA-A resolution, where the peak positive sidelobe is 52%.

in scale, until D array, where minor changes are made at the very center of the array.

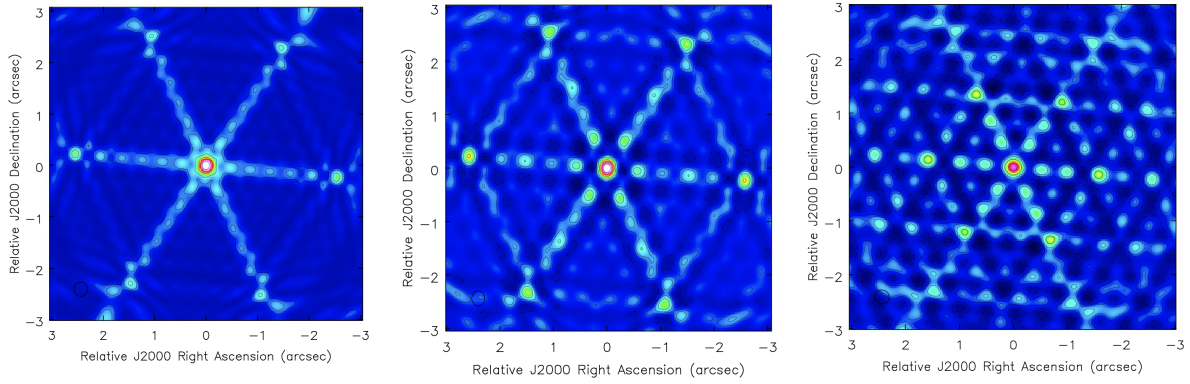


Figure 3: Left to right: point spread function for a 30min observation for the VLA A array with NA weighting, and VLA-F and VLA-G weighted to A array NA resolution. Contour levels are powerlaw in factor 2, starting at 5% of the peak of unity.

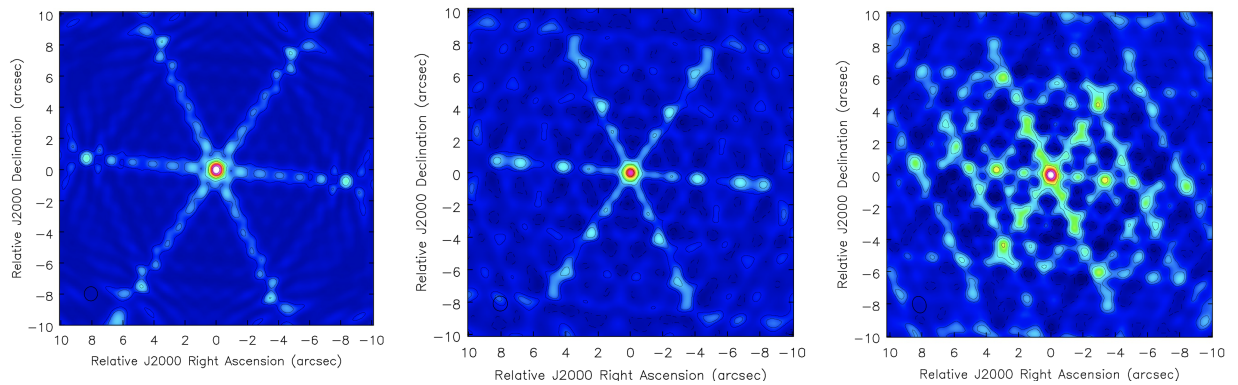


Figure 4: Left to right: point spread function for a 30min observation for the VLA B array, and VLA-F and VLA-G weighted to B array NA resolution. Contour levels are powerlaw in factor 2, starting at 5% of the peak of unity.

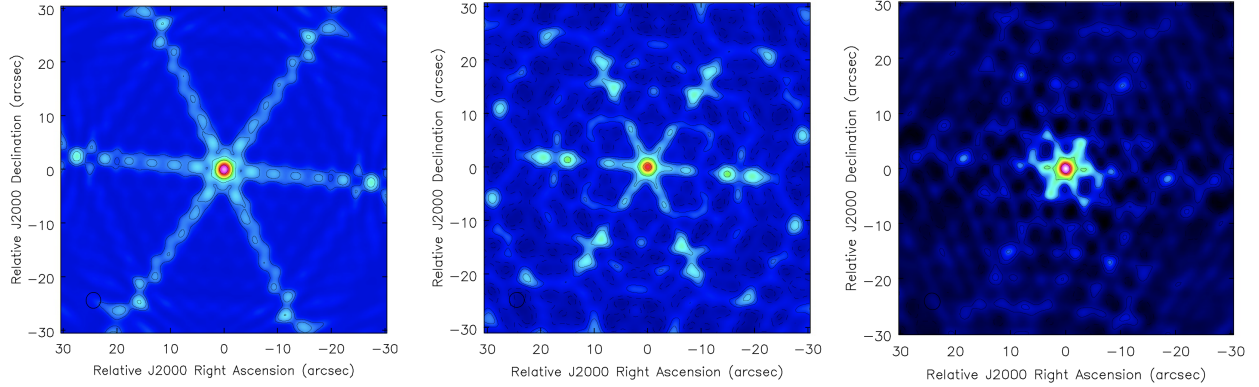


Figure 5: Left to right: point spread function for a 30min observation for the VLA C array, and VLA-F and VLA-G weighted to C array NA resolution. Contour levels are powerlaw in factor 2, starting at 5% of the peak of unity.

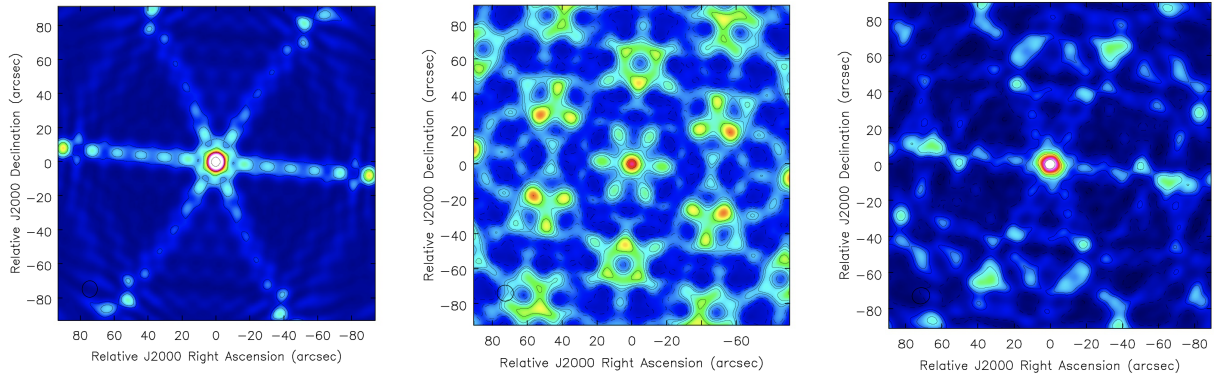


Figure 6: Left to right: point spread function for a 30min observation for the VLA D array, and VLA-F and VLA-G weighted to D array NA resolution. Contour levels are powerlaw in factor 2, starting at 5% of the peak of unity.

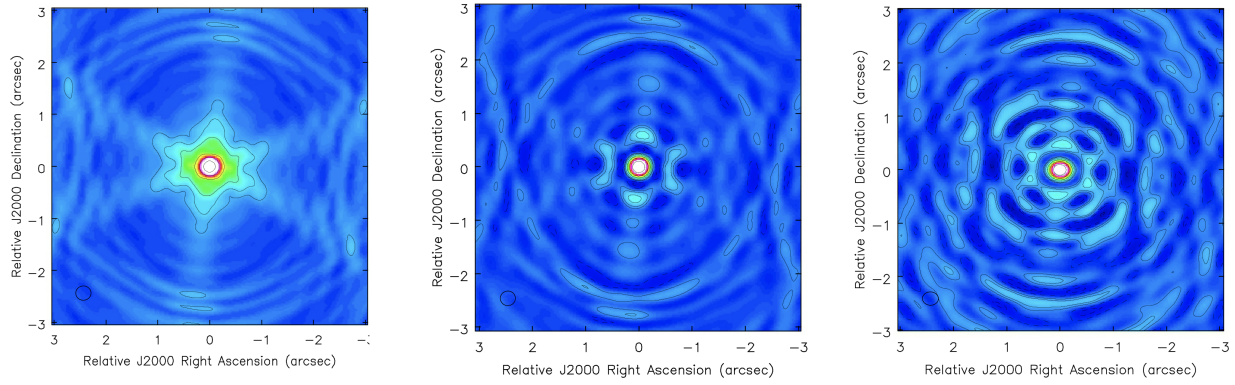


Figure 7: Left to right: point spread function for an 8 hour observation for the VLA A array, and VLA-F and VLA-G weighted to A array NA resolution. Contour levels are powerlaw in factor 2, starting at 1% of the peak of unity.

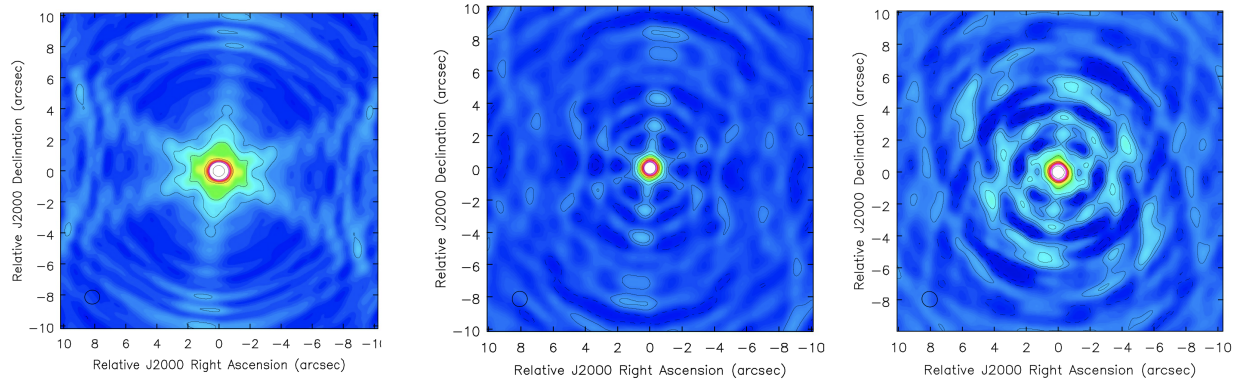


Figure 8: Left to right: point spread function for an 8 hour observation for the VLA B array, and VLA-F and VLA-G weighted to B array NA resolution. Contour levels are powerlaw in factor 2, starting at 1% of the peak of unity.

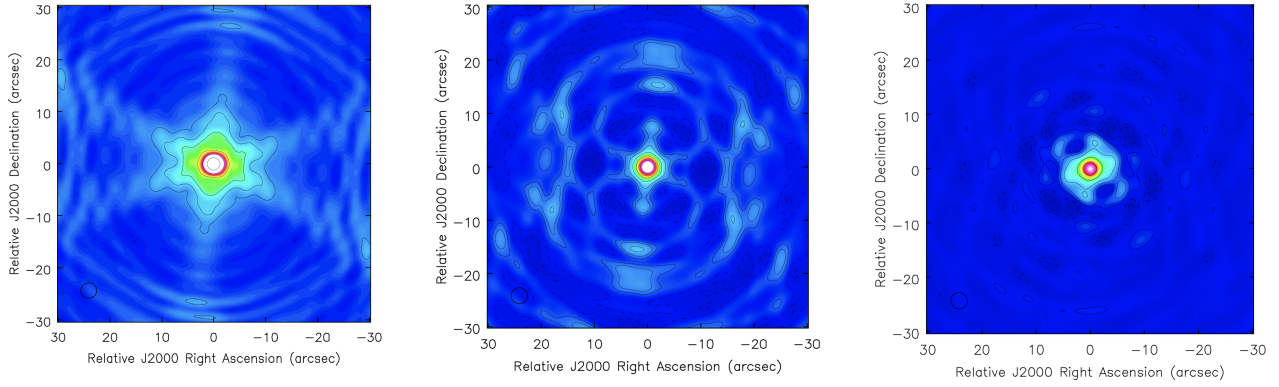


Figure 9: Left to right: point spread function for an 8 hour observation for the VLA C array, and VLA-F and VLA-G weighted to C array NA resolution. Contour levels are powerlaw in factor 2, starting at 1% of the peak of unity.

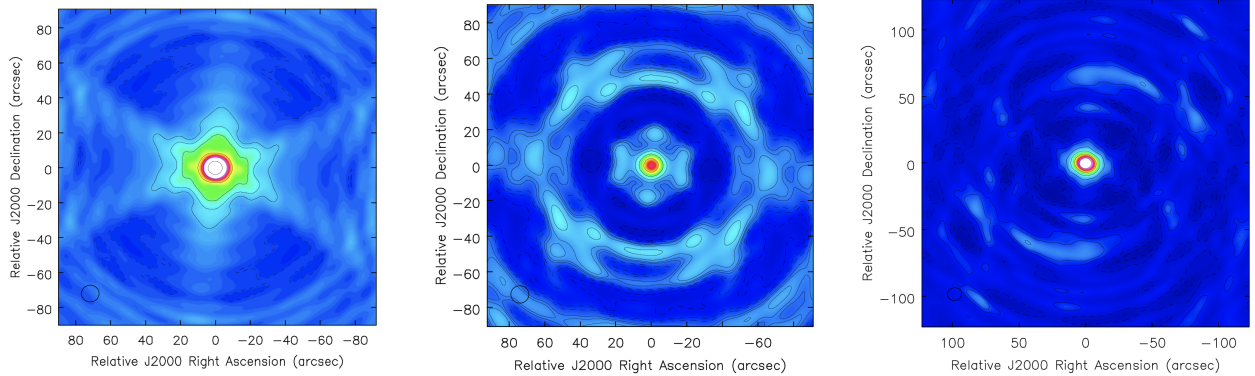


Figure 10: Left to right: point spread function for an 8 hour observation for the VLA D array, and VLA-F and VLA-G weighted to D array NA resolution. Contour levels are powerlaw in factor 2, starting at 1% of the peak of unity.

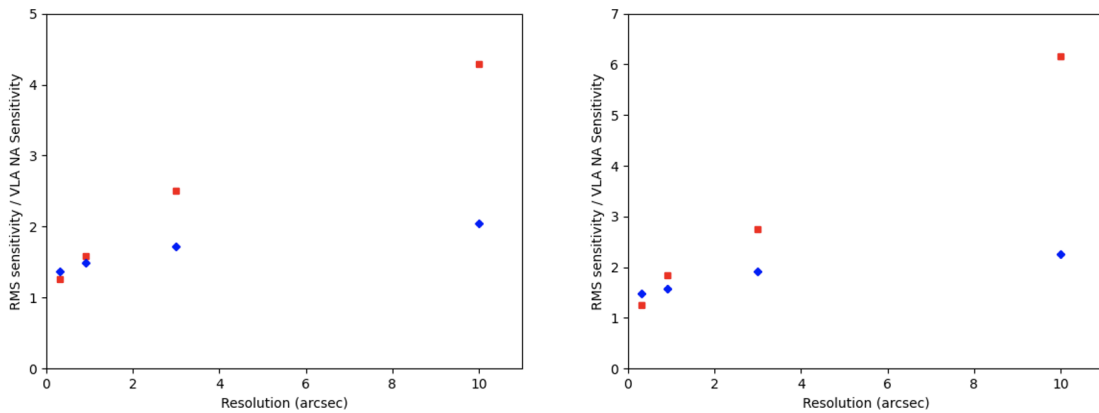


Figure 11: Left: rms sensitivity in 0.5 hours for VLA-F (red squares) and VLA-G (blue diamonds), normalized by the VLA NA weighted sensitivity for the given configuration/resolution. Right: same but for 8 hours.

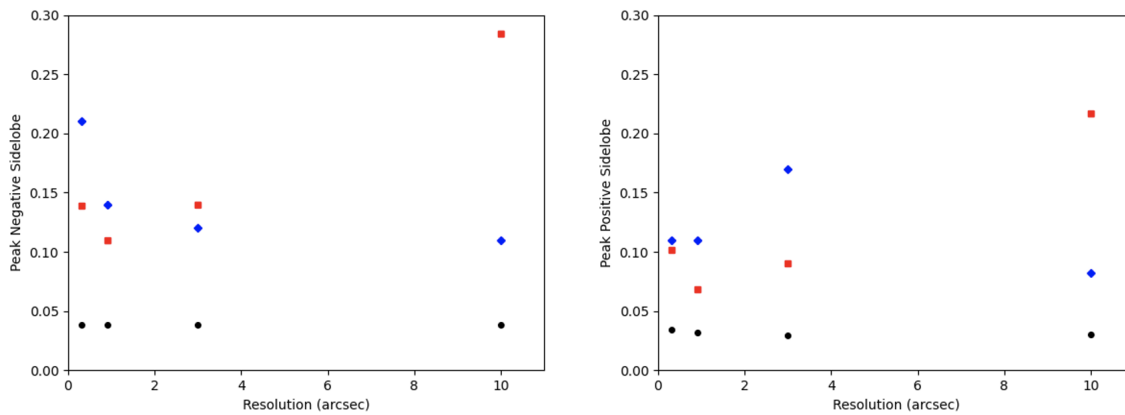


Figure 12: Left: peak positive sidelobe in 0.5 hours for VLA-ABCD (black circles), VLA-F (red squares), and VLA-G (blue diamonds). Right: same but for 8 hours.

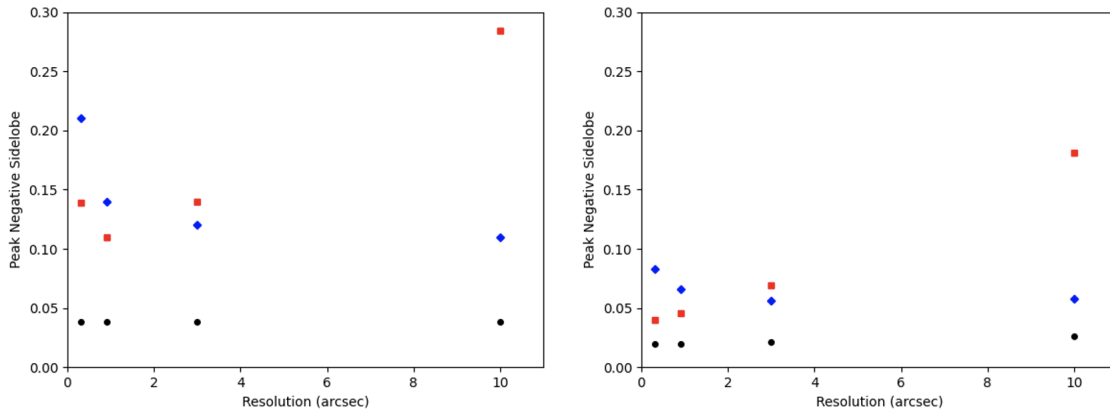


Figure 13: Left: peak negative sidelobe in 0.5 hours for VLA-ABCD (black circles), VLA-F (red squares), and VLA-G (blue diamonds). Right: same but for 8 hours.

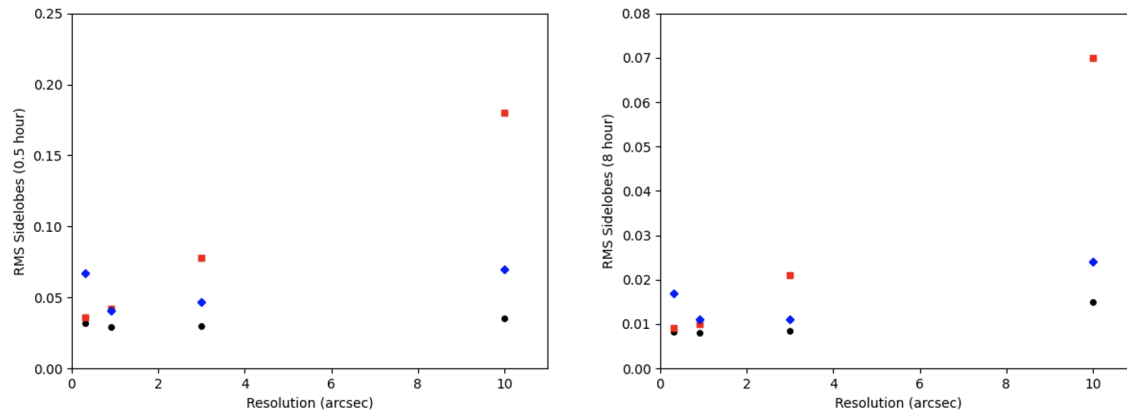


Figure 14: Left: rms of sidelobes from radii = 2x FWHM to 20x FWHM for 0.5 hours integration for VLA-ABCD (black circles), VLA-F (red squares), and VLA-G (blue diamonds). Right: same but for 8 hours.

4 Conclusions

I have considered the question: how well does a mixed-scale configuration of the VLA involving baselines from D to A array, perform relative to the current individual VLA configurations? The goal is not to address a specific science priority, which is always evolving and hence premature, but to see what types of degradations are expected in noise performance and PSF quality when trying to span a large range of spatial frequencies with only 27 antennas. To do so, I have employed two representative configurations: one with an emphasis on longer spacings (VLA-F), and the second with better short spacing coverage (VLA-G).

In terms of thermal noise, VLA-F performs well for high resolution imaging, with an increase of only 26% relative to VLA-A. However, the performance degrades dramatically for low resolution science, with a factor 5 increase in noise at D-array resolution relative to VLA-D. VLA-G is somewhat worse than VLA-F at the A-array resolution (36% higher noise than VLA-A), but better at D array resolution (factor 2 higher noise than VLA-D).

In terms of the PSF, the negative and positive sidelobes are generally substantially larger for the mixed-scale configurations than the individual VLA A,B,C,D, arrays, by factors of 2 to 6, with the VLA-F performing better at VLA-A resolution relative to VLA-G, and conversely at VLA-D resolution, as expected. The PSF sidelobe rms values are comparable between VLA-F and A configuration (12%), but much worse relative to D configuration (factor 5). For VLA-G, the PSF rms sidelobes are a factor 2 higher relative to both A and D configuration.

Overall, it appears that getting within a factor 2, or better, of the thermal noise performance of individual current VLA configurations is plausible with a mixed-configuration covering a wide range in baselines. The PSF sidelobes seem more challenging, with performance degraded by factors of 2 up to 6. If the paramount science at the time of transition requires very high dynamic range imaging of complex fields, the PSF sidelobe level may become the primary selection criterion for choosing the final configuration.